

Chapter 5

The Kolmogorov Law of Turbulence

What Can Rigorously Be Proved? Part II

Roger Lewandowski and Benoît Pinier

Abstract We recall what are the different known solutions for the incompressible Navier-Stokes Equations, in order to fix a suitable functional setting for the probabilistic frame that we use to derive turbulence models, in particular to define the mean velocity and pressure fields, the Reynolds stress and eddy viscosities. Homogeneity and isotropy are discussed within this framework and we give a mathematical proof of the famous $-5/3$ Kolmogorov law, which is discussed in a numerical simulation performed in a numerical box with a non trivial topography on the ground.

MCS Classification : 76D05, 76F65, 65M60

5.1 Introduction

We focus in this paper on the law of the $-5/3$, which attracted a lot of attention from the fluid mechanics community these last decades, since it is a basis for many turbulence models, such as Large Eddy Simulation models (see for instance in [20, 21, 44, 50]). Although it is usually known as the Kolmogorov law, it seems that it appears for the first time in a paper by Onsager [42] in 1949, and not in the serie of papers published by Kolmogorov in 1941 (see in [56]), where the author focuses on the $2/3$'s law, by introducing the essential scales related to homogeneous and isotropic turbulent flows (see formula (5.33) below). In this major contribution to the field, Kolmogorov opened the way for the derivation of laws based on similarity principles such as the $-5/3$'s law (see also in [11, 32]).

R. Lewandowski • B. Pinier (✉)
IRMAR, UMR 6625, Université Rennes 1, and Fluminance Team INRIA, Campus Beaulieu,
35042 Rennes cedex, France
e-mail: Roger.Lewandowski@univ-rennes1.fr; benoit.pinier@inria.fr
<http://perso.univ-rennes1.fr/roger.lewandowski>

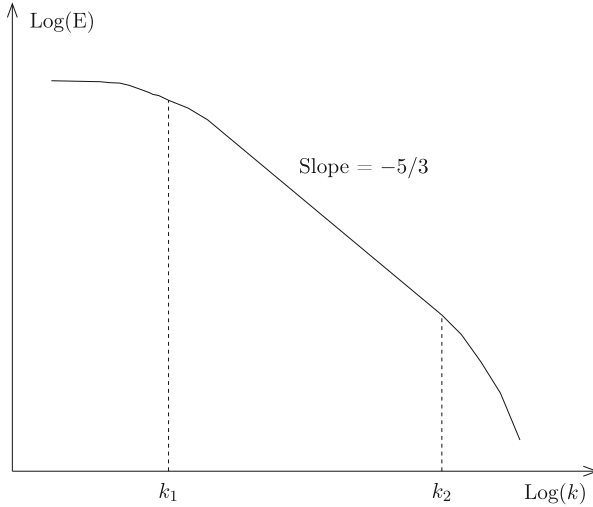


Fig. 5.1 Energy spectrum log-log curve

Roughly speaking, the $-5/3$'s law states that in some inertial range $[k_1, k_2]$, the energy density of the flow $E(k)$ behaves like $C^e k^{-5/3}$, where k denotes the current wave number [see Fig. 5.1 below and the specific law (5.40)].

This paper is divided in a theoretical part and a numerical part, in which we aim at:

1. carefully express what is the appropriate similarity assumption that must satisfy an homogeneous and isotropic turbulent flow in order to derive the $-5/3$'s law (Assumptions 5.4.1 and 5.4.2 below),
2. to theoretically derive the $-5/3$ law from the similarity assumption (see Theorem 5.4.2 below),
3. to discuss the numerical validity of such a law from a numerical simulation in a test case, using the software BENFLOW 1.0, developed at the Institute of Mathematical Research of Rennes.

Before processing items (1) and (2), we discuss on different results about the Navier-Stokes equations (5.1) (NSE in what follows), that are one of the main tools in fluid mechanics, as well as the Reynolds stress (5.13) derived by taking the expectation of the NSE, once the appropriate probabilistic frame is specified. We then define the density energy $E(k)$, which is the energy of the flow in the sphere $\{k = |\mathbf{k}|\}$ in the Fourier space. Furthermore, we introduce the concept of dimensional bases in order to properly set Assumptions 5.4.1 and 5.4.2.

The numerical simulation takes place in a computational box (see Fig. 5.2) with a non trivial topography (see Fig. 5.3), by using the mean NSE (5.12), the $k - \mathcal{L}$ model (5.20), and appropriate boundary conditions supposed to model the dynamics

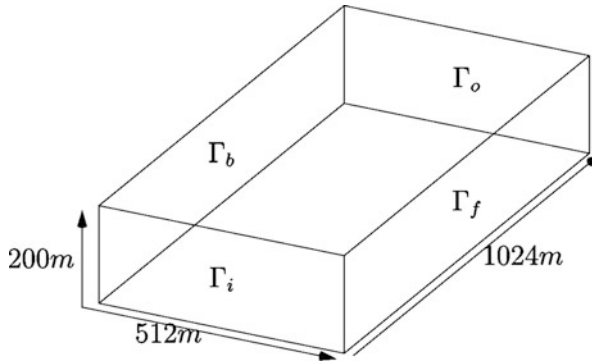


Fig. 5.2 Computational box

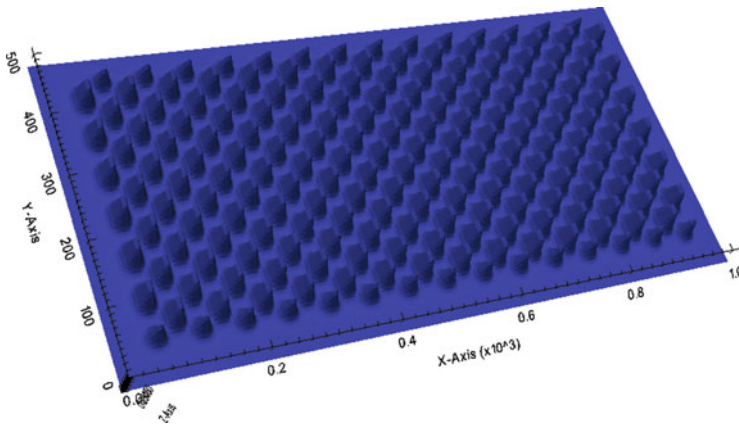


Fig. 5.3 View of the ground

of the atmospheric boundary layer. Atmospheric boundary layer modeling is a modern challenge because of its significance in climate change issues. We find in the literature many simulations carried out in different configurations, such as for example the case of a flat ground [1, 5, 13, 45], the case of stable or convective boundary layers [38, 59], urban simulations where building are modeled by parallelipeds [39], wind farms [46], realistic configurations including mountains [37, 58]. Of course, this flows is not homogeneous nor isotropic. However, the simulations shows that the curve of $\log_{10}(E(k))$ exhibits an inertial range over 4 decades, in which the regression straight line has a slope equal to $-2.1424 \neq -5/3$ (see Fig. 5.6), suggesting that the $-5/3$'s law is not satisfied in this case.

5.2 About the 3D Navier Stokes Equations

5.2.1 Framework

Let $\Omega \subseteq \mathbb{R}^3$ be a C^1 bounded convex smooth domain, Γ its boundary, $T \in \mathbb{R}_+$ (eventually $T = +\infty$), and $Q = [0, T] \times \Omega$. The velocity of the flow is denoted by \mathbf{v} , its pressure by p . The incompressible Navier Stokes equation satisfied by (\mathbf{v}, p) (NSE in the remainder) are as follows:

$$\left\{ \begin{array}{ll} \partial_t \mathbf{v} + (\mathbf{v} \cdot \nabla) \mathbf{v} - \nabla \cdot (2\nu D\mathbf{v}) + \nabla p = \mathbf{f} & \text{in } Q, & \text{(i)} \\ \nabla \cdot \mathbf{v} = 0 & \text{in } Q, & \text{(ii)} \\ \mathbf{v} = 0 & \text{on } \Gamma, & \text{(iii)} \\ \mathbf{v} = \mathbf{v}_0 & \text{at } t = 0, & \text{(iv)} \end{array} \right. \quad (5.1)$$

where \mathbf{v}_0 is any divergence free vector fields such that $\mathbf{v}_0 \cdot \mathbf{n}|_{\Gamma} = 0$, $\nu > 0$ denotes the kinematic viscosity, that we suppose constant for the simplicity, \mathbf{f} is any external force (such as the gravity for example), $D\mathbf{v}$ denotes the deformation tensor, $\nabla \cdot$ the divergence operator and $(\mathbf{v} \cdot \nabla) \mathbf{v}$ is the nonlinear transport term, specifically

$$\begin{aligned} D\mathbf{v} &= \frac{1}{2} (\nabla \mathbf{v} + \nabla \mathbf{v}^t), \quad \nabla \mathbf{v} = (\partial_j v_i)_{1 \leq i, j \leq 3}, \quad \mathbf{v} = (v_1, v_2, v_3), \quad \partial_i = \partial \partial x_i, \\ \nabla \cdot \mathbf{v} &= \partial_i v_i, \\ [(\mathbf{v} \cdot \nabla) \mathbf{v}]_i &= v_j \partial_j v_i, \end{aligned}$$

by using the Einstein summation convention. We recall that it is easily deduced from the incompressibility condition (see [11]):

$$\begin{aligned} (\mathbf{v} \cdot \nabla) \mathbf{v} &= \nabla \cdot (\mathbf{v} \otimes \mathbf{v}), \quad \mathbf{v} \otimes \mathbf{v} = (v_i v_j)_{1 \leq i, j \leq 3}, \\ \nabla \cdot (2\nu D\mathbf{v}) &= \nu \Delta \mathbf{v}. \end{aligned}$$

In the following, we will consider the functional spaces

$$\mathbf{W} = \{\mathbf{v} \in H_0^1(\Omega)^3, \nabla \cdot \mathbf{v} = 0\} \leftrightarrow \mathbf{V} = \{\mathbf{v} \in L^2(\Omega)^3, \mathbf{v} \cdot \mathbf{n}|_{\Gamma} = 0, \nabla \cdot \mathbf{v} = 0\}, \quad (5.2)$$

Throughout the paper, we assume $\mathbf{v}_0 \in \mathbf{V}$.

5.2.2 Strong Solutions to the NSE

Let P be the orthogonal projection $L^2(\Omega)^3 \hookrightarrow \mathbf{V}$, A and F the operators

$$A\mathbf{v} = -\nu P \Delta \mathbf{v}, \quad F\mathbf{v} = P((\mathbf{v} \cdot \nabla) \mathbf{v}).$$

By applying P to (5.1.i) in noting that $P(\nabla p) = 0$, we are led to the following initial value problem

$$\begin{cases} \frac{d\mathbf{v}}{dt} = -A\mathbf{v} + F\mathbf{v} + P\mathbf{f}(t), & \text{(i)} \\ \mathbf{v}(0) = \mathbf{v}_0, & \text{(ii)} \end{cases} \quad (5.3)$$

where $t \rightarrow \mathbf{v}(t)$ and $t \rightarrow \mathbf{f}(t)$ are considered as functions valued in \mathbf{W} and \mathbf{V} respectively.

Definition 5.2.1 We say that $\mathbf{v} = \mathbf{v}(t)$ is a strong solution to the NSE in a time interval $[0, T^*]$ if $d\mathbf{v}/dt$ and $A\mathbf{v}$ exist and are continuous in $[0, T^*]$ and (5.3.i) is satisfied there.

Remark 5.2.1 In Definition 5.2.1, the pressure is not involved. It can be reconstructed by the following equation

$$\Delta p = -\nabla \cdot ((\mathbf{v} \cdot \nabla) \mathbf{v}) + \nabla \cdot \mathbf{f}, \quad (5.4)$$

derived from Eq. (5.1.i) by taking its divergence.

The existence of a strong solution is proved in Fujita-Kato [18]. It is subject to regularity conditions regarding the initial data \mathbf{v}_0 and the source \mathbf{f} . The result is stated as follows.

Theorem 5.2.1 *We assume*

- (i) $\mathbf{v}_0 \in \mathbf{V} \cap H^{1/2}(\Omega)^3$,
- (ii) \mathbf{f} is Hölder continuous in $[0, T]$.

Then there exists $T^ = T^*(\nu, \|\mathbf{v}_0\|_{1/2,2,\Omega}, \|\mathbf{f}\|_{C^{0,\alpha}(\Omega)})$ such that the NSE admits a unique strong solution $\mathbf{v} = \mathbf{v}(t)$. Moreover, if $\mathbf{f} = \mathbf{f}(t, \mathbf{x})$ is Hölder continuous in $Q = [0, T^*] \times \Omega$, then $\mathbf{v}(t, \mathbf{x})$, $\nabla \mathbf{v}(t, \mathbf{x})$, $\Delta \mathbf{v}(t, \mathbf{x})$ and $\partial \mathbf{v}(t, \mathbf{x})/\partial t$ are Hölder continuous in $]0, T^*[\times \Omega$.*

Remark 5.2.2 The strong solution is solution of the equation

$$\mathbf{v}(t) = e^{-tA} \mathbf{v}_0 - \int_0^t e^{-(t-s)A} F(\mathbf{v}(s)) ds + \int_0^t e^{-(t-s)A} P\mathbf{f}(s) ds, \quad (5.5)$$

which is approached by the sequence $(\mathbf{v}_n)_{n \in \mathbb{N}}$ expressed by

$$\mathbf{v}_n(t) = e^{-tA} \mathbf{v}_0 - \int_0^t e^{-(t-s)A} F(\mathbf{v}_{n-1}(s)) ds + \int_0^t e^{-(t-s)A} P\mathbf{f}(s) ds, \quad (5.6)$$

The reader is referred to [9, 12, 28] for more details concerning the question of strong solutions.

5.2.3 Turbulent Solutions

Definition 5.2.2 We say that \mathbf{v} is a turbulent solution of NSE (5.1) in $[0, T]$ if

- (i) $\mathbf{v} \in L^2([0, T], \mathbf{W}) \cap L^\infty([0, T], L^2(\Omega))$,
- (ii) $\partial_t \mathbf{v} \in L^{4/3}([0, T], \mathbf{W}') = [L^4([0, T], \mathbf{W})]'$ (by writing $\partial_t = \frac{\partial}{\partial t}$ for the simplicity),
- (iii) $\lim_{t \rightarrow 0} \|\mathbf{v}(\cdot, t) - \mathbf{v}_0(\cdot)\|_{0,2,\Omega} = 0$,
- (iv) $\forall \mathbf{w} \in L^4([0, T], \mathbf{W})$,

$$\begin{aligned} & \int_0^T \langle \partial_t \mathbf{v}, \mathbf{w} \rangle dt + \int_0^T \int_\Omega (\mathbf{v} \otimes \mathbf{v}) : \nabla \mathbf{w} \, dx dt + \int_0^T \int_\Omega \nabla \mathbf{v} : \nabla \mathbf{w} \, dx dt \\ & = \int_0^T \langle \mathbf{f}, \mathbf{w} \rangle dt, \end{aligned}$$

where for $\mathbf{u} \in \mathbf{W}$, $\mathbf{F} \in \mathbf{W}'$, $\langle \mathbf{F}, \mathbf{u} \rangle$ denotes the duality pairing between \mathbf{F} and \mathbf{u} ,

- (v) \mathbf{v} satisfies the energy inequality at each $t > 0$,

$$\frac{1}{2} \int_\Omega |\mathbf{v}(t, \mathbf{x})|^2 dx + \nu \int_0^t \int_\Omega |\nabla \mathbf{v}(t', \mathbf{x})|^2 dx dt' \leq \int_0^t \langle \mathbf{f}, \mathbf{v} \rangle dt'.$$

Remark 5.2.3 Once again, the pressure is not involved in this formulation. In this frame, it is recovered by the De Rham Theorem (see for instance in [55]).

The existence of a turbulent solution was first proved by Leray [29] in the whole space, then by Hopf [22] in the case of a bounded domain with the no slip boundary condition, which is the case under consideration here. This existence result can be stated as follows.

Theorem 5.2.2 Assume that $\mathbf{v}_0 \in \mathbf{V}$, $\mathbf{f} \in L^{4/3}([0, T], \mathbf{W}')$. Then the NSE (5.1) has a turbulent solution.

Remark 5.2.4 The turbulent solution is global in time, which means that it may be extended to $t \in [0, \infty[$ depending on a suitable assumption on \mathbf{f} . However it is not known whether it is unique or not. Moreover, it is not known if the energy inequality is an equality.

The reader is also referred to [14, 16, 36, 55] for further results on turbulent (also weak) solutions of the NSE.

5.3 Mean Navier-Stokes Equations

5.3.1 Reynolds Decomposition

Based on strong or turbulent solutions, it is known that it is possible to set a probabilistic framework in which we can decompose the velocity \mathbf{v} and the pressure as a the sum of the statistical mean and a fluctuation, namely

$$\mathbf{v} = \bar{\mathbf{v}} + \mathbf{v}', \quad p = \bar{p} + p'. \quad (5.7)$$

More generally, any tensor field ψ related to the flow can be decomposed as

$$\psi = \bar{\psi} + \psi'. \quad (5.8)$$

The statistical filter is linear and subject to satisfy the Reynolds rules:

$$\overline{\partial_t \psi} = \partial_t \bar{\psi}, \quad (5.9)$$

$$\overline{\nabla \psi} = \nabla \bar{\psi}, \quad (5.10)$$

as well as

$$\overline{\overline{\psi}} = \bar{\psi} \text{ leading to } \overline{\psi'} = 0. \quad (5.11)$$

We have studied in [11] different examples of such filters. Historically, such a decomposition was first considered in works by Stokes [53], Boussinesq [6], Reynolds [49], Prandtl [47], in the case of the « long time average »(see also in [31]). Later on, Taylor [54], Kolmogorov [25] and Onsager [42] have considered such decompositions when the fields related to the flow are considered as random variables, which was one of the starting point for the development of modern probability theory.

5.3.2 Reynolds Stress and Closure Equations

We take the mean of the NSE (5.1) by using (5.9)–(5.11). We find out the following system:

$$\begin{cases} \partial_t \bar{\mathbf{v}} + (\bar{\mathbf{v}} \cdot \nabla) \bar{\mathbf{v}} - \nu \Delta \bar{\mathbf{v}} + \nabla \bar{p} = -\nabla \cdot \boldsymbol{\sigma}^{(r)} + \mathbf{f} & \text{in } Q, \\ \nabla \cdot \bar{\mathbf{v}} = 0 & \text{in } Q, \\ \bar{\mathbf{v}} = 0 & \text{on } \Gamma, \\ \bar{\mathbf{v}} = \bar{\mathbf{v}}_0 & \text{at } t = 0, \end{cases} \quad (5.12)$$

where

$$\boldsymbol{\sigma}^{(R)} = \overline{\mathbf{v}' \otimes \mathbf{v}'} \quad (5.13)$$

is the Reynolds stress. The big deal in turbulence modeling is to express $\boldsymbol{\sigma}^{(R)}$ in terms of averaged quantities. The most popular model is derived from the Boussinesq assumption which consists in writing:

$$\boldsymbol{\sigma}^{(R)} = -\nu_t D\bar{\mathbf{v}} + \frac{2}{3}k \text{Id}, \quad (5.14)$$

where

1. $k = \frac{1}{2} \text{tr} \boldsymbol{\sigma}^{(R)} = \frac{1}{2} \overline{|\mathbf{v}'|^2}$ is the turbulent kinetic energy (TKE),
2. ν_t is an eddy viscosity.

In order to close the system, the eddy viscosity remains to be modeled. To do so, many options are available (see in [4, 10, 11, 24, 26, 30, 40, 50]).

One of the most popular model is the Smagorinsky's model (see for instance in [20, 21, 24, 34, 44, 48, 50–52]), in which

$$\nu_t = C_s \delta^2 |D\mathbf{v}|, \quad (5.15)$$

where $C_s \approx 0.1$ or 0.2 is an universal dimensionless constant, and δ a characteristic scale, ideally the size of the smallest eddies in the flow the model is supposed to catch. This model is the foundation of the wide class of Large Eddy Simulation models. The reader will find various mathematical results concerning the Smagorinsky's model in [3, 11, 24, 35, 43].

We next mention the so-called TKE model, given by

$$\nu_t = C_k \ell \sqrt{k}, \quad (5.16)$$

which gives accurate results for the simulation of realistic flows (see for instance [33]). In model (5.16), ℓ denotes the Prandtl mixing length, C_k is a dimensionless constant that must be fixed according to experimental data. In practice, ℓ is taken to be equal to the local mesh size in a numerical simulation, and k is computed by using the closure equation (see in [11, 40])

$$\partial_t k + \bar{\mathbf{v}} \cdot \nabla k - \nabla \cdot (\nu_t \nabla k) = \nu_t |D\bar{\mathbf{v}}|^2 - \frac{k\sqrt{k}}{\ell}. \quad (5.17)$$

The reader will find a bunch of mathematical result concerning the coupling of the TKE equation to the mean NSE in [7, 8, 11, 19, 27, 30].

Finally, we mention the famous $k - \mathcal{E}$ model that is used for the numerical simulations carried out in Sect. 5.5. In this model, \mathcal{E} denotes the turbulent dissipation

$$\mathcal{E} = 2\nu \overline{|D\mathbf{v}'|^2}, \quad (5.18)$$

and dimensional analysis leads to write

$$\nu_t = C_\mu \frac{k^2}{\mathcal{E}}. \quad (5.19)$$

The coupled system used to compute k and \mathcal{E} is the following (see [11, 40] for the derivation of these equations):

$$\begin{cases} \partial_t k + \bar{\mathbf{v}} \cdot \nabla k - \nabla \cdot (\nu_t \nabla k) = \nu_t |D\bar{\mathbf{v}}|^2 - \mathcal{E}. \\ \partial_t \mathcal{E} + \bar{\mathbf{v}} \cdot \nabla \mathcal{E} - \nabla \cdot (\nu_t \nabla \mathcal{E}) = c_\eta k |D\bar{\mathbf{v}}|^2 - c_\mathcal{E} \frac{\mathcal{E}^2}{k}, \end{cases} \quad (5.20)$$

where $C_\nu = 0.09$, $c_\mathcal{E} = 1.92$ and $c_\eta = 1.44$ are dimensionless constants.

5.4 Law of the $-5/3$

The idea behind the law of the $-5/3$ for homogeneous and isotropic turbulence is that in the « inertial range », the energy density $E = E(k)$ at a given point (t, \mathbf{x}) is driven by the dissipation \mathcal{E} . In this section, we properly define the energy density E for homogeneous and isotropic turbulent flows. We then set the frame of the dimensional bases and the similarity principle in order to rigorously derive the law of the $-5/3$.

Remark 5.4.1 For homogeneous and isotropic turbulence, one can show the identity $\mathcal{E} = 2\nu |D\bar{\mathbf{v}}|^2 = 2\nu |D\mathbf{v}|^2$ (see in [11]).

5.4.1 Energy Density of the Flow

Roughly speaking, homogeneity and isotropy means that the correlations in the flows are invariant under translations and isometries (see in [2, 11, 32]), which we assume throughout this section, as well as the stationarity of the mean flow for simplicity. Let

$$\mathbb{E} = \frac{1}{2} \overline{|\mathbf{v}|^2}, \quad (5.21)$$

be the total mean kinetic energy at a given point $\mathbf{x} \in \Omega$, which we not specify in what follows.

Theorem 5.4.1 *There exists a measurable function $E = E(k)$, defined over \mathbb{R}_+ , the integral of which over \mathbb{R}_+ is finite, and such that*

$$\mathbb{E} = \int_0^\infty E(k)dk. \quad (5.22)$$

Proof Let \mathbb{B}_2 be the two order correlation tensor expressed by:

$$\mathbb{B}_2 = \mathbb{B}_2(\mathbf{r}) = \overline{(v_i(\mathbf{x})v_j(\mathbf{x} + \mathbf{r}))}_{1 \leq i, j \leq 3} = (B_{ij}(\mathbf{r}))_{1 \leq i, j \leq 3}, \quad (5.23)$$

which only depend on \mathbf{r} by the homogeneity assumption, nor on t because of the stationarity assumption. It is worth noting that

$$\mathbb{E} = \frac{1}{2} \text{tr} \mathbb{B}_2(0). \quad (5.24)$$

Let $\widehat{\mathbb{B}}_2$ denotes the Fourier transform of \mathbb{B} expressed by

$$\forall \mathbf{k} \in \mathbb{R}^3, \quad \widehat{\mathbb{B}}_2(\mathbf{k}) = \frac{1}{(2\pi)^3} \int_{\mathbb{R}^3} \mathbb{B}_2(\mathbf{r}) e^{-i\mathbf{k}\cdot\mathbf{r}} d\mathbf{r}, \quad (5.25)$$

We deduce from the Plancherel formula,

$$\forall \mathbf{r} \in \mathbb{R}^3, \quad \mathbb{B}_2(\mathbf{r}) = \frac{1}{(2\pi)^3} \int_{\mathbb{R}^3} \widehat{\mathbb{B}}_2(\mathbf{k}) e^{i\mathbf{k}\cdot\mathbf{r}} d\mathbf{k}, \quad (5.26)$$

which makes sense for both types of solutions to the NSE, strong or turbulent (see the Sect. 5.2). It is easily checked that the isotropy of \mathbb{B}_2 in \mathbf{r} yields the isotropy of $\widehat{\mathbb{B}}_2$ in \mathbf{k} . Therefore, according to Theorem 5.1 in [11] we deduce the existence of two real valued functions \widetilde{B}_d and \widetilde{B}_n of class C^1 such that¹

$$\forall \mathbf{k} \in \mathbb{R}^3, \quad |\mathbf{k}| = k, \quad \widehat{\mathbb{B}}_2(\mathbf{k}) = (\widetilde{B}_d(k) - \widetilde{B}_n(k)) \frac{\mathbf{k} \otimes \mathbf{k}}{k^2} + \widetilde{B}_n(k) \mathbf{I}_3. \quad (5.27)$$

Using formula (5.27) yields

$$\widehat{B}_{ii}(\mathbf{k}) = \widetilde{B}_d(k) + 2\widetilde{B}_n(k), \quad (5.28)$$

which combined with Fubini's Theorem, (5.24) and (5.26), leads to

$$\int_{\mathbb{R}^3} \widehat{B}_{ii}(\mathbf{k}) d\mathbf{k} = \int_0^\infty \left(\int_{|\mathbf{k}|=k} \widehat{B}_{ii}(\mathbf{k}) d\sigma \right) dk = \int_0^\infty 4\pi k^2 (\widetilde{B}_d(k) + 2\widetilde{B}_n(k)) dk, \quad (5.29)$$

¹ k already denotes the TKE, and from now also the wavenumber, $k = |\mathbf{k}|$. This is commonly used in turbulence modeling, although it might sometimes be confusing.

by noting $d\sigma$ the standard measure over the sphere $\{|\mathbf{k}| = k\}$. This proves the result, where $E(k)$ is given by

$$E(k) = \left(\frac{k}{2\pi}\right)^2 (\widetilde{B}_d(k) + 2\widetilde{B}_n(k)). \quad (5.30)$$

□

Remark 5.4.2 From the physical point of view, $E(k)$ is the amount of kinetic energy in the sphere $S_k = \{|\mathbf{k}| = k\}$. As such, it is expected that $E \geq 0$ in \mathbb{R} , and we deduce from (5.22) that $E \in L^1(\mathbb{R}_+)$. Unfortunately, we are not able to prove that $E \geq 0$ from formula (5.30), which remains an open problem.

5.4.2 Dimensional Bases

Only length and time are involved in this frame, since we do not consider heat transfers and the fluid is incompressible. Therefore, any field ψ related to the flow has a dimension $[\psi]$ encoded as:

$$[\psi] = (\text{length})^{d_\ell(\psi)} (\text{time})^{d_\tau(\psi)}, \quad (5.31)$$

which we express through the couple

$$\mathbb{D}(\psi) = (d_\ell(\psi), d_\tau(\psi)) \in \mathbb{Q}^2. \quad (5.32)$$

Definition 5.4.1 A length-time basis is a couple $b = (\lambda, \tau)$, where λ is a given constant length and τ a constant time.

Definition 5.4.2 Let $\psi = \psi(t, \mathbf{x})$ (constant, scalar, vector, tensor...) be defined on $Q = [0, T] \times \Omega$. Let ψ_b be the dimensionless field defined by:

$$\psi_b(t', \mathbf{x}') = \lambda^{-d_\ell(\psi)} \tau^{-d_\tau(\psi)} \psi(\tau t', \lambda \mathbf{x}'),$$

where

$$(t', \mathbf{x}') \in Q_b = \left[0, \frac{T}{\tau}\right] \times \frac{1}{\lambda} \Omega,$$

is dimensionless. We say that $\psi_b = \psi_b(t', \mathbf{x}')$ is the b -dimensionless field deduced from ψ .

5.4.3 Kolmogorov Scales

Let us consider the length-time basis $b_0 = (\lambda_0, \tau_0)$, given by

$$\lambda_0 = \nu^{\frac{3}{4}} \mathcal{E}^{-\frac{1}{4}}, \quad \tau_0 = \nu^{\frac{1}{2}} \mathcal{E}^{-\frac{1}{2}}, \quad (5.33)$$

where \mathcal{E} is the dissipation defined by (5.18) (see also Remark 5.4.1). The scale λ_0 is known as the Kolmogorov scale. The important point here is that

$$\mathcal{E}_{b_0} = \nu_{b_0} = 1. \quad (5.34)$$

Moreover, for all wave number k , and because

$$\mathbb{D}(E) = (3, -2), \quad (5.35)$$

we get

$$E(k) = \lambda_0^3 \tau_0^{-2} E_{b_0}(\lambda_0 k) = \nu^{\frac{5}{4}} \mathcal{E}^{\frac{1}{4}} E_{b_0}(\lambda_0 k), \quad (5.36)$$

by using (5.33). We must determine the universal profile E_{b_0} .

5.4.4 Proof of the $-5/3$'s Law

The law of the $-5/3$ is based on two assumptions about the flow:

1. the separation of the scales (Assumption 5.4.1 below),
2. the similarity assumption (Assumption 5.4.2 below).

Assumption 5.4.1 *Let ℓ be the Prandtl mixing length. Then*

$$\lambda_0 \ll \ell. \quad (5.37)$$

Assumption 5.4.2 *There exists an interval*

$$[k_1, k_2] \subset \left[\frac{2\pi}{\ell}, \frac{2\pi}{\lambda_0} \right] \text{ s.t. } k_1 \ll k_2 \text{ and on } [\lambda_0 k_1, \lambda_0 k_2],$$

$$\forall b_1 = (\lambda_1, \tau_1), b_2 = (\lambda_2, \tau_2) \text{ s.t. } \mathcal{E}_{b_1} = \mathcal{E}_{b_2}, \text{ then } E_{b_1} = E_{b_2}. \quad (5.38)$$

Theorem 5.4.2 *Scale separation and similarity Assumptions 5.4.1 and 5.4.2 yield the existence of a constant C such that*

$$\forall k' \in [\lambda_0 k_1, \lambda_0 k_2] = J_r, \quad E_{b_0}(k') = C(k')^{-\frac{5}{3}}. \quad (5.39)$$

Corollary 5.4.1 *The energy spectrum satisfies the $-5/3$ law*

$$\forall k \in [k_1, k_2], \quad E(k) = C \mathcal{E}^{\frac{2}{3}} k^{-\frac{5}{3}}, \quad (5.40)$$

where C is a dimensionless constant.

Proof Let

$$b^{(\alpha)} = (\alpha^3 \lambda_0, \alpha^2 \tau_0).$$

As

$$\mathcal{E}_{b^{(\alpha)}} = 1 = \mathcal{E}_{b_0},$$

the similarity assumption yields

$$\forall k' \in J_r, \quad \forall \alpha > 0, \quad E_{b^{(\alpha)}}(k') = E_{b_0}(k'),$$

which leads to the functional equation,

$$\forall k' \in J_r, \quad \forall \alpha > 0, \quad \frac{1}{\alpha^5} E_{b_0}(k') = E_{b_0}(\alpha^3 k'),$$

whose unique solution is given by

$$\forall k' \in J_r, \quad E_{b_0}(k') = C(k')^{-\frac{5}{3}}, \quad C = \left(\frac{k_1}{\lambda_0} \right)^{\frac{5}{3}} E_0 \left(\frac{k_1}{\lambda_0} \right),$$

hence the result. Corollary 5.4.1 is a direct consequence of (5.36) combined with (5.39).

Remark 5.4.3 It can be shown that the law of $-5/3$ yields the Smagorinsky's model (5.15) (see in [11]).

5.5 Numerical Experiments

5.5.1 Simulation Setting

The computational domain Ω is a box, the size $L_x \times L_y \times L_z$ of which is equal to (1024 m, 512 m, 200 m) (see Fig. 5.3). The number of nodes is (256, 128, 64). The bottom of the box, plotted in Fig. 5.3, has a non trivial topography modeled by gaussian smooth domes, the height of which being equal to 50 m. We perform the simulation with $\nu = 2 \times 10^{-5} \text{ m}^2 \text{ s}^{-1}$, which yields a Reynolds number equal

to 9.10^7 . We use the mean NSE with the Boussinesq assumption, coupled to the $k - \mathcal{E}$ model, namely the PDE system (5.12)–(5.14)–(5.19)–(5.20). We specify in what follows the boundary conditions, by considering the following decomposition of $\Gamma = \partial\Omega$:

$$\Gamma = \Gamma_t \cup \Gamma_f \cup \Gamma_b \cup \Gamma_g \cup \Gamma_i \cup \Gamma_o,$$

where

- Γ_t is the top of the box,
- Γ_f is the front face,
- Γ_b is the back face,
- Γ_g is the bottom of the box (the ground),
- Γ_i is the inlet,
- Γ_o is the outlet.

The condition on Γ_i is prescribed by the Monin Obukhov similitude law [41]:

$$\mathbf{v}(x, y, z, t)|_{\Gamma_i} = \left(\frac{u_\star}{\kappa} \ln \left(\frac{z + z_0}{z_0} \right), 0, 0 \right)^t, \quad (5.41)$$

where $\kappa = 0.4$ is the Von Karman constant, z denotes the distance from the ground level, the aerodynamic roughness length z_0 is equal to 0.1 m, the friction velocity is expressed by:

$$u_\star = \kappa U_{ref} \left[\ln \left(\frac{H_{ref} + z_0}{z_0} \right) \right]^{-1}, \quad (5.42)$$

by taking $U_{ref} = 36 \text{ ms}^{-1}$ and $H_{ref} = 200 \text{ m}$. The turbulent kinetic energy and turbulent dissipation are setted by

$$\begin{cases} k|_{\Gamma_i} = u_\star^{1/2} C_v^{-1/2}, \\ \mathcal{E}|_{\Gamma_i} = \frac{u_\star^3}{\kappa(z + z_0)}. \end{cases} \quad (5.43)$$

On Γ_b , velocity, TKE and turbulent dissipation are subject to verify the no slip and homogeneous boundary conditions,

$$\begin{cases} \mathbf{v}|_{\Gamma_g} = (0, 0, 0)^t, \\ k|_{\Gamma_g} = 0, \\ \mathcal{E}|_{\Gamma_g} = 0. \end{cases} \quad (5.44)$$

On the top and lateral boundaries, we put

$$\begin{cases} \mathbf{v} \cdot \mathbf{n} = 0 & \text{on } \Gamma_t \cup \Gamma_b \cup \Gamma_f, \\ \nabla k \cdot \mathbf{n} = 0 & \text{on } \Gamma_t \cup \Gamma_b \cup \Gamma_f, \\ \nabla \mathcal{E} \cdot \mathbf{n} = 0 & \text{on } \Gamma_t \cup \Gamma_b \cup \Gamma_f. \end{cases} \quad (5.45)$$

Finally a null gradient condition is prescribed at the outlet Γ_o

$$\begin{cases} \nabla(\mathbf{v} \cdot \mathbf{n}) = 0 & \text{on } \Gamma_o, \\ \nabla k \cdot \mathbf{n} = 0 & \text{on } \Gamma_o, \\ \nabla \mathcal{E} \cdot \mathbf{n} = 0 & \text{on } \Gamma_o. \end{cases} \quad (5.46)$$

Remark 5.5.1 The PDE system (5.12)–(5.14)–(5.19)–(5.20) with the boundary conditions (5.41)–(5.43)–(5.44)–(5.45)–(5.46) yields a very hard mathematical problem. The existence and the uniqueness of a solution is a difficult issue, whether for global weak solutions or local time strong solutions.

5.5.2 Results

The numerical scheme we use for the simulation is based on the standard finite volume method (FVM) in space, and an Implicit Euler for the time discretization. For the simplicity, we will not write here this technical part of the work. The reader will find comprehensive presentations of the FVM in [15, 17, 23, 57].

The simulation reaches a statistical equilibrium in about 180 physical seconds, which is the time at which the results are displayed. In Figs. 5.4 and 5.5, are plotted the values of the streamwise and spanwise components of the velocity at $z = 50$ m, which corresponds to the dome height.

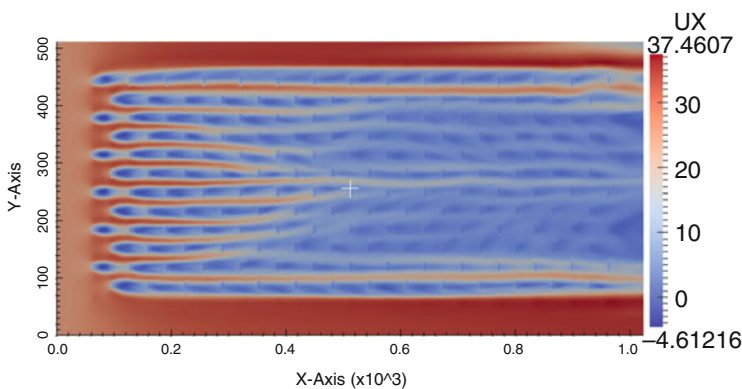


Fig. 5.4 Streamwise direction of the flow at the $z = 50$ m cutplane

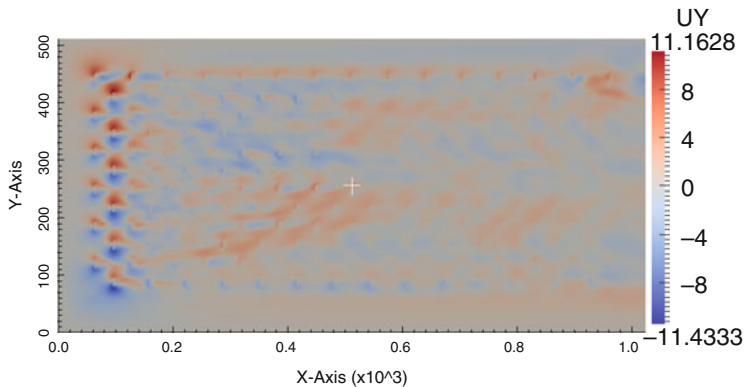


Fig. 5.5 Spanwise direction at the $z = 50$ m cutplane

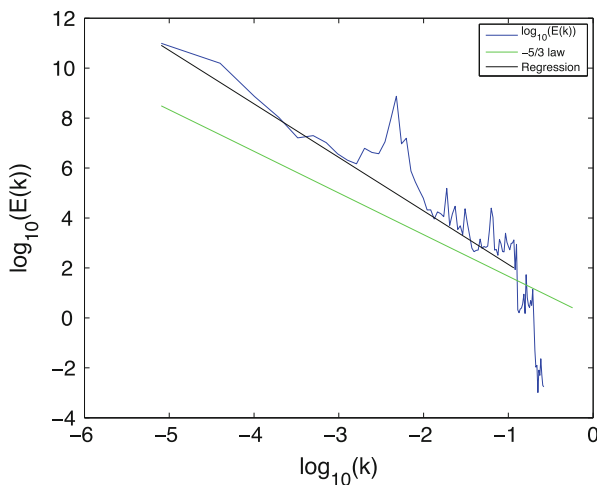


Fig. 5.6 Energy spectrum at the point $(x, y, z) = (500, 200, 50)$

In Fig. 5.6, we have plotted the energy spectrum of the flow at $(x, y, z) = (500, 200, 50)$ using a log-log scale, together with a straight line whose slope is equal to $-5/3 = -1,666\dots$ and the regression straight line of $\log_{10}(E(k))$, whose slope is about equal to -2.1424 . The results call for the following comments.

1. The simulation reveals a certain reliability of the code, which suggests the convergence of the numerical method. However, the mathematical convergence of the scheme remains an open question, closely related to the question of the existence of solutions mentioned in Remark 5.5.1.
2. The curve $\log_{10}(E(k))$ is an irregular curve which substantially differs from a straight line, so that we cannot conclude that numerically $E(k)$ behaves like $C^{te}k^\alpha$ in some interval $[k_1, k_2]$. Moreover, there is a gap between the slope of

the regression straight line of the curve and $-5/3$. However, something that looks like an inertial range can be identified between $k = 10^{-5} \text{ m}^{-1}$ and $k = 10^{-1} \text{ m}^{-1}$. This departure from the $-5/3$ law asks for the following comments and questions.

- The case under consideration yields a turbulence which is not homogeneous nor isotropic, which may explain the slope equal to -2.1424 we found.
- This simulation does not validate the Kolmogorov law or any law like $E(k) \approx C^* k^\alpha$. We cannot infer that such a law holds or not. Many parameters may generate the oscillations we observe in the curve $\log_{10}(E(k))$, such as any eventual numerical dissipation, a wrong choice of the constants in the $k - \mathcal{E}$ model which also may be not accurate, the boundary conditions we used and which may be questionable.

References

1. D. Apsley, I. Castro, A limited-length-scale k-epsilon model for the neutral and stably-stratified atmospheric boundary layer. *Bound.-Layer Meteorol.* **83**(1), 75–98 (1997)
2. G.K. Batchelor, *The Theory of Homogeneous Turbulence*. Cambridge Monographs on Mechanics and Applied Mathematics (Cambridge University Press, New York, 1959)
3. H. Beirão da Veiga, On the Ladyzhenskaya-Smagorinsky turbulence model of the Navier-Stokes equations in smooth domains. The regularity problem. *J. Eur. Math. Soc.* **11**(1), 127–167 (2009)
4. L.C. Berselli, T. Iliescu, W.J. Layton, *Mathematics of Large Eddy Simulation of Turbulent Flows*. Scientific Computation (Springer, Berlin, 2006)
5. E. Bou-Zeid, Large-eddy simulation of neutral atmospheric boundary layer flow over heterogeneous surfaces: blending height and effective surface roughness. *Water Resour. Res.* **40**(2), 1–18 (2004)
6. J. Boussinesq, Essai sur la théorie des eaux courantes. Mémoires présentés par divers savants à l'Académie des Sciences **23**(1), 1–660 (1877)
7. F. Brossier, R. Lewandowski, Impact of the variations of the mixing length in a first order turbulent closure system. *Math. Model. Numer. Anal.* **36**(2), 345–372 (2002)
8. M. Bulíček, R. Lewandowski, J. Málek, On evolutionary Navier-Stokes-Fourier type systems in three spatial dimensions. *Comment. Math. Univ. Carolin.* **52**(1), 89–114 (2011)
9. M. Cannone, Harmonic analysis tools for solving the incompressible Navier-Stokes equations, in *Handbook of Mathematical Fluid Dynamics*, vol. III (North-Holland, Amsterdam, 2004), pp. 161–244
10. T. Chacón-Rebollo, R. Lewandowski, A variational finite element model for large-eddy simulations of turbulent flows. *Chin. Ann. Math. Ser. B* **34**(5), 667–682 (2013)
11. T. Chacón Rebollo, R. Lewandowski, *Mathematical and Numerical Foundations of Turbulence Models and Applications*. Modeling and Simulation in Science, Engineering and Technology (Birkhäuser/Springer, New York, 2014)
12. J.-Y. Chemin, I. Gallagher, Wellposedness and stability results for the Navier-Stokes equations in \mathbf{R}^3 . *Ann. Inst. H. Poincaré Anal. Non Linéaire* **26**(2), 599–624 (2009)
13. F.K. Chow, R.L. Street, M. Xue, J.H. Ferziger, Explicit filtering and reconstruction turbulence modeling for large-eddy simulation of neutral boundary layer flow. *J. Atmos. Sci.* **62**, 2058–2077 (2005)
14. P. Constantin, C. Foias, *Navier-Stokes Equations*. Chicago Lectures in Mathematics (University of Chicago Press, Chicago, IL, 1988)

15. R. Eymard, T. Gallouët, R. Herbin, Finite volume methods, in *Solution of Equation in R^n (Part 3), Techniques of Scientific Computing (Part 3)*. Handbook of Numerical Analysis, vol. 7 (Elsevier, Amsterdam, 2000), pp. 713–1018
16. E. Feireisl, *Dynamics of Viscous Compressible Fluids*. Oxford Lecture Series in Mathematics and its Applications, vol. 26 (Oxford University Press, Oxford, 2004)
17. J.H. Ferziger, M. Peric, *Computational Methods for Fluid Dynamics* (Springer Science & Business Media, Berlin, 2012)
18. H. Fujita, T. Kato, On the Navier-Stokes initial value problem. i. Arch. Ration. Mech. Anal. **16**(4), 269–315 (1964)
19. T. Gallouët, J. Lederer, R. Lewandowski, F. Murat, L. Tartar, On a turbulent system with unbounded eddy viscosities. Nonlinear Anal. **52**(4), 1051–1068 (2003)
20. M. Germano, Fundamentals of large eddy simulation, in *Advanced Turbulent Flow Computations (Udine, 1998)*. CISM Courses and Lectures, vol. 395 (Springer, Vienna, 2000), pp. 81–130
21. M. Germano, U. Piomelli, P. Moin, W. Cabot, A dynamic subgrid-scale eddy viscosity model. Phys. Fluids A **3**(7), 1760–1765 (1991)
22. E. Hopf, Über die Anfangswertaufgabe für die hydrodynamischen Grundgleichungen. Math. Nachr. **4**(1–6), 213–231 (1950). doi:10.1002/mana.3210040121. <http://dx.doi.org/10.1002/mana.3210040121>
23. H. Jasak, *Error Analysis and Estimation for the Finite Volume Method with Applications to Fluid Flows* (Imperial College London [University of London], London, 1996)
24. V. John, *Large Eddy Simulation of Turbulent Incompressible Flows: Analytical and numerical results for a class of LES models*. Lecture Notes in Computational Science and Engineering, vol. 34 (Springer, Berlin, 2004)
25. A.N. Kolmogorov, The local structure of turbulence in incompressible viscous fluid for very large Reynolds' numbers. Dokl. Akad. Nauk SSSR **30**, 301–305 (1941)
26. B.E. Launder, D.B. Spalding, The numerical computation of turbulent flows. Comput. Methods Appl. Mech. Eng. **3**(2), 269–289 (1974)
27. J. Lederer, R. Lewandowski, A RANS 3D model with unbounded eddy viscosities. Ann. Inst. H. Poincaré Anal. Non Linéaire **24**(3), 413–441 (2007)
28. P.-G. Lemarié-Rieusset, *Recent Developments in the Navier-Stokes Problem*. Chapman & Hall/CRC Research Notes in Mathematics, vol. 431 (Chapman & Hall/CRC, Boca Raton, FL, 2002)
29. J. Leray, Sur le mouvement d'un liquide visqueux emplissant l'espace. Acta Math. **63**(1), 193–248 (1934)
30. R. Lewandowski, The mathematical analysis of the coupling of a turbulent kinetic energy equation to the Navier-Stokes equation with an eddy viscosity. Nonlinear Anal. **28**(2), 393–417 (1997)
31. R. Lewandowski, Long-time turbulence model deduced from the Navier-Stokes equations. Chin. Ann. Math. Ser. B **36**(5), 883–894 (2015)
32. R. Lewandowski, *The Kolmogorov-Taylor Law of Turbulence: What can Rigorously be Proved?* Handbook of Applications of Chaos Theory (Taylor and Francis, London, 2016)
33. R. Lewandowski, G. Pichot, Numerical simulation of water flow around a rigid fishing net. Comput. Methods Appl. Mech. Eng. **196**(45–48), 4737–4754 (2007)
34. D.K. Lilly, Numerical simulation and prediction of atmospheric convection, in *Mécanique des Fluides Numérique (Les Houches, 1993)* (North-Holland, Amsterdam, 1996), pp. 325–374
35. J.-L. Lions, *Quelques Méthodes de Résolution des Problèmes aux Limites Non linéaires* (Dunod, Gauthier-Villars, 1969)
36. P.-L. Lions, *Mathematical Topics in Fluid Mechanics: Incompressible Models*, vol. 1. Oxford Lecture Series in Mathematics and its Applications, vol. 3 (Clarendon Press, Oxford University Press, Oxford, New York, 1996)
37. N. Marjanovic, S. Wharton, F.K. Chow, Investigation of model parameters for high-resolution wind energy forecasting: case studies over simple and complex terrain. J. Wind Eng. Ind. Aerodyn. **134**, 10–24 (2014)

38. P.J. Mason, Large-eddy simulation of the convective atmospheric boundary layer. *J. Atmos. Sci.* **46**, 1492–1516 (1989)
39. T. Michioka, A. Sato, K. Sada, Large-eddy simulation coupled to mesoscale meteorological model for gas dispersion in an urban district. *Atmos. Environ.* **75**(x), 153–162 (2013)
40. B. Mohammadi, O. Pironneau, *Analysis of the k-Epsilon Turbulence Model*. Research in Applied Mathematics (Wiley, Masson, Chichester, 1994)
41. A.S. Monin, A.M. Obukhov, Basic laws of turbulent mixing in the surface layer of the atmosphere. *Contrib. Geophys. Inst. Acad. Sci. USSR* **24**(151), 163–187 (1954)
42. L. Onsager, Statistical hydrodynamics. *Nuovo Cimento* (9) **6**(Supplemento, 2(Convegno Internazionale di Meccanica Statistica)), 279–287 (1949)
43. C. Pares Madroñal, Étude mathématique et approximation numérique de quelques problèmes aux limites de la mécanique des fluides incompressibles. Institut National de Recherche en Informatique et en Automatique (INRIA), Rocquencourt (1992)
44. S.B. Pope, *Turbulent Flows* (Cambridge University Press, Cambridge, 2000)
45. F. Porté-Agel, C. Meneveau, M.B. Parlange, A scale-dependent dynamic model for large-eddy simulation: application to a neutral atmospheric boundary layer. *J. Fluid Mech.* **415**, 261–284 (2000)
46. F. Porté-Agel, Y.-T. Wu, H. Lu, R.J. Conzemius, Large-eddy simulation of atmospheric boundary layer flow through wind turbines and wind farms. *J. Wind Eng. Ind. Aerodyn.* **99**(4), 154–168 (2011). The Fifth International Symposium on Computational Wind Engineering
47. L. Prandtl, über die ausgebildeten turbulenz. *Zeitschrift für angewandte Mathematik und Mechanik* **5**, 136–139 (1925)
48. L. Prandtl, *Prandtl—Essentials of Fluid Mechanics*, 3rd edn., vol. 158. Applied Mathematical Sciences (Springer, New York, 2010). Translated from the 12th German edition by Katherine Asfaw and edited by Herbert Oertel, With contributions by P. Erhard, D. Etling, U. Müller, U. Riedel, K.R. Sreenivasan, J. Warnatz
49. O. Reynolds, An experimental investigation of the circumstances which determine whether the motion of water shall be direct or sinuous, and of the law of resistance in parallel channels. *Philos. Trans. R. Soc.* **174**, 935–982 (1883)
50. P. Sagaut, *Large Eddy Simulation for Incompressible Flows*, 3rd edn. Scientific Computation (Springer, Berlin, 2006). An introduction, Translated from the 1998 French original, With forewords by Marcel Lesieur and Massimo Germano, With a foreword by Charles Meneveau
51. J. Smagorinsky, On the application of numerical methods to the solution of systems of partial differential equations arising in meteorology, in *Frontiers of Numerical Mathematics* (University of Wisconsin Press, Madison, WI, 1960), pp. 107–125
52. J. Smagorinsky, General circulation experiments with the primitive equations. *Mon. Weather Rev.* **93**(3), 99 (1963)
53. G.G. Stokes, On the effect of the internal friction of fluids on the motion of pendulums. *Trans. Cambridge Philos. Soc.* **9**, 8–106 (1851)
54. G.I. Taylor, Statistical theory of turbulence. part i-iv. *Proc. Roy. Soc. A* **151**, 421–478 (1935)
55. R. Temam, *Navier-Stokes Equations* (AMS Chelsea Publishing, Providence, RI, 2001). Theory and numerical analysis, Reprint of the 1984 edition
56. V.M. Tikhomirov, in *Selected Works of A.N. Kolmogorov: Volume I: Mathematics and Mechanics*, ed. by V.M. Tikhomirov (Kluwer Academic Publishers, Dordrecht, Boston, London, 1992)
57. H.G. Weller, G. Tabor, H. Jasak, C. Fureby, A tensorial approach to computational continuum mechanics using object-oriented techniques. *Comput. Phys.* **12**(6), 620–631 (1998)
58. B. Zhou, F.K. Chow, Nested large-eddy simulations of the intermittently turbulent stable atmospheric boundary layer over real terrain. *J. Atmos. Sci.* **71**(3), 1021–1039 (2014)
59. B. Zhou, J.S. Simon, F.K. Chow, The convective boundary layer in the terra incognita. *J. Atmos. Sci.* **71**, 2545–2563 (2014)